

Article

Use of Bioprinted Lipases in Microwave-Assisted Esterification Reactions

Jéssica Jéssi Carvalho de Melo¹, Gardenia Laís Passos da Silva¹, Danyelle Andrade Mota¹ ,
Luma Mirely de Souza Brandão¹ , Ranyere Lucena de Souza^{1,2} , Matheus M. Pereira³ , Álvaro Silva Lima^{1,2}
and Cleide Mara Faria Soares^{1,2,*} 

¹ UNIT, Tiradentes University, Av. Murilo Dantas, 300, Farolândia, Aracaju 49032-490, SE, Brazil

² ITP, Institute of Technology and Research, Av. Murilo Dantas, 300, Farolândia, Aracaju 49032-490, SE, Brazil

³ CICECO, Aveiro Institute of Materials, Chemistry Department, University of Aveiro, 3810-193 Aveiro, Portugal

* Correspondence: cleide18@yahoo.com.br; Tel.: +55-(79)-32182115 or +55-(79)-32182190

Abstract: In this study, a comparative evaluation was performed in batch esterification reactions under conventional heating (CH) and assisted by microwave irradiation (MW) using bioprinted lipases. Microwave-irradiation-assisted reactions generally provide higher productivities and improve synthesis performance in terms of increased rate and reduced reaction times, resulting in higher interest yields in less time. Productivity was calculated with the enzymes: *Burkholderia cepacia* lipase (BCL), *Candida rugosa* lipase (CRL), and porcine pancreas lipase (PPL) using different fatty acids (lauric acid (12:0), myristic acid (14:0), palmitic acid (16:0), stearic acid (18:0), and oleic acid (18:1)) and alcohols at a molar ratio of 1:8. The microwave reactor was operated at a temperature of 45 °C, and power varied between 50 W and 200 W. Bioprinted BCL (bBCL) showed the highest productivity among the tested lipases. In the reaction with the best result, bBCL with lauric acid under MW, the reaction time decreased from 24 h (CH) to 25 min (MW) and the productivity increased 33 times compared with the reactions under CH. The increase in productivity demonstrates its activation that occurred as a result of conformational changes of the enzyme in the bioprinting process, confirmed by Fourier transform infrared (FTIR) spectrometric analysis, which reduces the content of bBCL α -helix with lauric acid. The biocatalyst showed high operational stability over eight cycles, while losing only 19% of its initial activity with half-life times of 12.8 batches. The storage time was five weeks, maintaining $\approx 80\%$ activity. The results demonstrate the prospect of a new enzymatic route to obtain hyperactive catalysts, with the use of bioprinted lipases in esterification reactions under microwave irradiation, for the synthesis of esters with a view to large-scale industrial application.

Keywords: bioprinting; microwave; esterification reaction



Citation: Carvalho de Melo, J.J.; Passos da Silva, G.L.; Mota, D.A.; de Souza Brandão, L.M.; de Souza, R.L.; Pereira, M.M.; Lima, Á.S.; Soares, C.M.F. Use of Bioprinted Lipases in Microwave-Assisted Esterification Reactions. *Catalysts* **2023**, *13*, 299. <https://doi.org/10.3390/catal13020299>

Academic Editor: Jose M. Guisan

Received: 23 December 2022

Revised: 17 January 2023

Accepted: 25 January 2023

Published: 28 January 2023



Copyright: © 2023 by the authors. Licensee MDPI, Basel, Switzerland. This article is an open access article distributed under the terms and conditions of the Creative Commons Attribution (CC BY) license (<https://creativecommons.org/licenses/by/4.0/>).

1. Introduction

Heating by microwave irradiation (MW) is based on the interaction of matter with the electric field of the incident radiation, causing the movement of ions and induced or permanent dipoles of the molecules, which orient themselves in the direction of the field. Because of the frequency, this movement occurs about a million times per second, causing friction of the molecules, resulting in the dissipation of electromagnetic energy from the field in the form of heat and temperature increase [1]. The literature reports that the heat produced by molecular friction induced in microwave-assisted chemical reactions, when compared with other techniques, improves the performance of synthesis in terms of increasing the reaction rate and reducing reaction times, resulting in greater achievement of products of interest in less time [2].

Furthermore, microwave-irradiation-assisted reactions can include the application of catalysts or biocatalysts to improve performance in different reactions [3–6]. Lipases have an intense dipole moment because of functional groups, which is attributed to their polar

nature [7]. Microwaves influence polar molecules, increasing friction and collisions between them, which can induce conformational changes in the lipase structure that facilitate the access of substrate molecules to the active site, making the enzyme more active, increasing speed, reducing reaction times, and improving conversion rates [8]. The synergism between MW and biocatalysis shows good results in esterification reactions [9]. Jaiswal and Rathod [10] studied the effect of MW on the synthesis of ethyl laurate, observing a conversion of 98% in 10 min, while under conventional heating (CH), a conversion of 92% was achieved in 4 h. Nhivekar and Rathod [11] obtained 85% conversion of polyethylene glycol stearate when using MW in 70 min. In CH, this conversion was only reached in 6 h. Liow et al. [12] reviewed technologies for intensifying the synthesis of biodiesel through enzymatic esterification reactions and demonstrated an improvement in terms of yield and reaction rate, with reduced enzymatic load and energy consumption in reactions under MW.

To expand the applicability of enzymes and replace synthesis routes that use chemical catalysts and organic solvents, studies indicate the development of methodologies that promote interfacial activation, such as molecular bioprinting, a strategy used to improve enzyme activity and promote biocatalyst hyperactivation [13,14]. Bioimprinting is an effective strategy that improves the catalytic performance of enzymes in nonaqueous medium. This technique promotes conformational changes in the enzyme when imprint molecules are added and interact with the active site of the enzyme. These molecules are then removed, but the enzyme does not return to its former conformation because of its rigid structure. After removal, the conformational structure of the bioprinted enzyme resembles the active “open lid” conformation of the biocatalysts, and an imprint containing functional groups capable of chemical interaction remains on the printed biocatalyst [14–16]. Owing to characteristics such as solvent tolerance, super activation, high stability, substrate specificity, enantioselectivity, and reuse, the use of bioprinted enzymes is a promising alternative in biotechnological processes [17]. Brandão et al. [18] observed a 70-fold increase in enzymatic activity of lauric acid bioprinted *Burkholderia cepacia* lipase (BCL) compared with unprinted BCL. According to Gao et al. [19], BCL bioprinted with fatty acids showed an increase in activity of 95%.

A novel path for the enzymatic synthesis is the association of bioprinting with MW. Thus, enzyme bioprinting in the esterification reaction under MW can become a promising trend for obtaining hyperactive catalysts applied in esterification reactions for the synthesis of esters. In this context, the present study presents an innovative aspect, as it seeks to evaluate the production of biocatalysts by the bioprinting technique and their application in microwave-assisted reactions, as no studies have reported the combined effect of bioprinted lipases with fatty acids in microwave-assisted esterification reactions.

2. Results and Discussion

2.1. Productivity Calculation

Initially, the productivity of bioprinted lipases was evaluated in the reactions under CH (Figure 1) and assisted by MW (Figures 2–4) as a strategy to increase catalytic efficiency.

For the productivity results under CH (Figure 1), BCL showed higher productivity for fatty acids in the following order: lauric acid (12:0)—6438.10 $\mu\text{mol/h}\cdot\text{mg}$ > myristic acid (14:0)—6266.62 $\mu\text{mol/h}\cdot\text{mg}$ > palmitic acid (16:0)—4835.94 $\mu\text{mol/h}\cdot\text{mg}$. It was observed that the productivity of bioprinted BCL (bBCL) increased approximately 6500 times for lauric acid compared with studies by Melo et al. [20] that evaluated the catalytic efficiency of unprinted lipases in esterification reactions under CH. This increase is related to the bioprinting of the enzyme, which promoted greater ease of access of the fatty acid to the lipase active site in the reaction mixture. In BCL, lauric acid has a greater preference for printing on the active site, as it is the only one that interacts with two amino acids that constitute the catalytic triad of this lipase [18]. The same profile was observed by Mukherjee and Gupta [21] when the *Thermomyces lanuginosus* lipase was bioprinted with surfactant to open the lid that covers the active site of the lipase, and 99% of biodiesel was obtained from soybean oil in about 4 h.

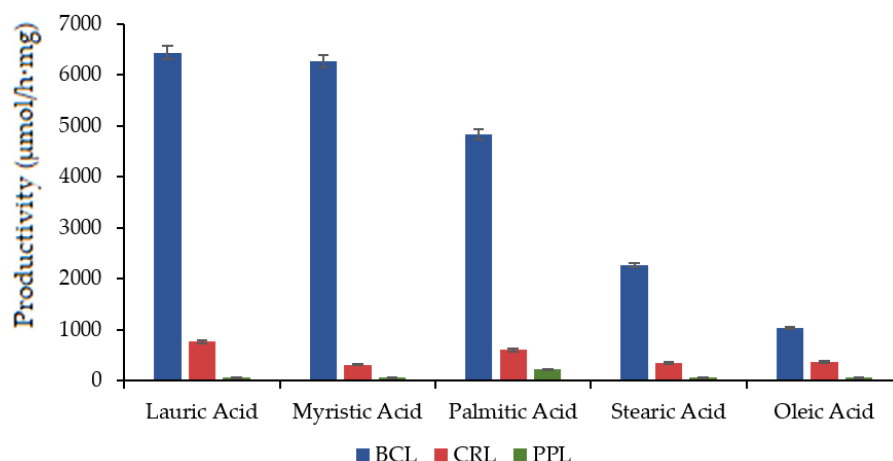


Figure 1. Productivity of *Burkholderia cepacia* lipase (BCL), *Candida rugosa* lipase (CRL), and porcine pancreas lipase (PPL) bioprinted with different fatty acids (lauric acid (12:0), myristic acid (14:0), palmitic acid (16:0), stearic acid (18:0), and oleic acid (18:1)) under conventional heating (CH) at 45 °C for 24 h.

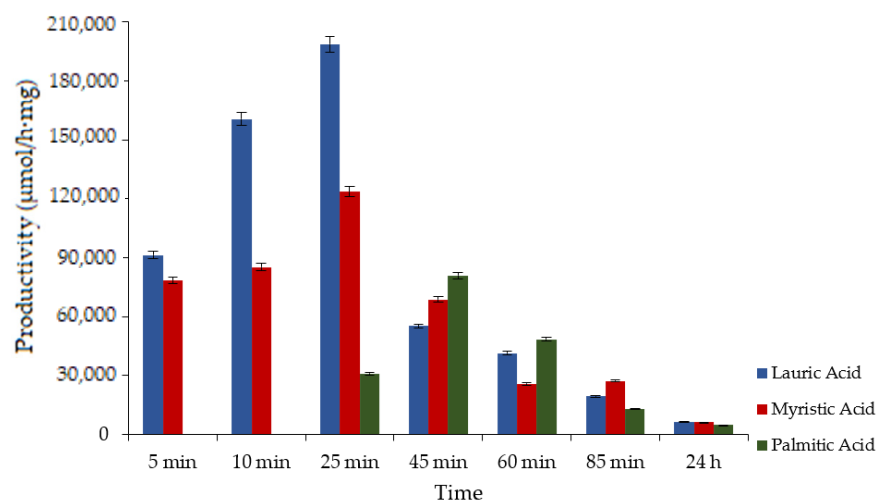


Figure 2. Productivity of BCL bioprinted with lauric acid (12:0), myristic acid (14:0), and palmitic acid (16:0) under MW (50 W) (5 min to 85 min) and under CH (24 h) at 45 °C.

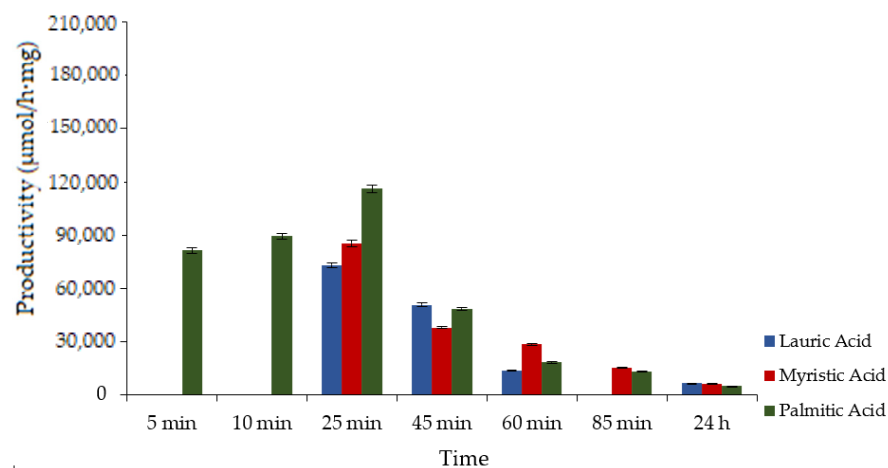


Figure 3. Productivity of BCL bioprinted with lauric acid (12:0), myristic acid (14:0), and palmitic acid (16:0) under MW (100 W) (5 min to 85 min) and under CH (24 h) at 45 °C.

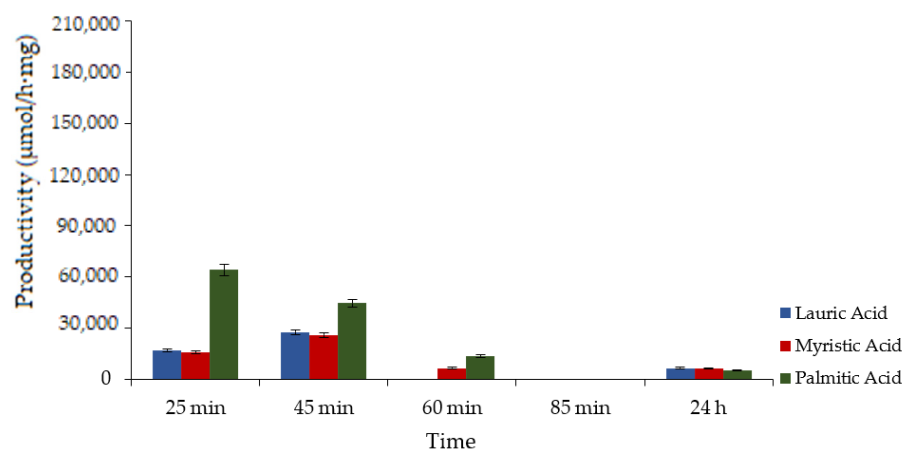


Figure 4. Productivity of BCL bioprinted with lauric acid (12:0), myristic acid (14:0), and palmitic acid (16:0) under MW (200 W) (5 min to 85 min) and under CH (24 h) at 45 °C.

To evaluate the potential of MW in the esterification reactions using bioprinted lipases, the best results of the reactions under CH (BCL with lauric acid, myristic acid, and palmitic acid; Figure 1) were evaluated. The results of the productivity of the BCL bioprinted with lauric acid, myristic acid, and palmitic acid in the powers of 50 W, 100 W, and 200 W can be seen in Figures 2–4, respectively.

For the esterification reactions of the bioprinted lipases under MW with 50 W of power (Figure 2), the time was varied from 5 min to 85 min. According to the results, BCL showed the highest productivity for lauric acid at the reaction time of 25 min (198,661.73 µmol/h·mg), with a productivity increase of approximately 33 times compared with the reactions under CH and a reduced reaction time from 24 h (CH) to 25 min (MW). Then, the highest productivity was for myristic acid with 25 min of reaction (123,614.43 µmol/h·mg), with an increase in productivity of 19 times compared with the reactions under CH and a reduced reaction time of 25 min (MW). For palmitic acid, the highest productivity was with 45 min of reaction (96,718.74 µmol/h·mg).

Productivity decreases when there is an increase in the length of fatty acid chains. The same profile for bioprinting was observed by Brandão et al. [18] under mild conditions. The effects on esters of different chain lengths as acyl donors in MW-assisted synthesis using BCL indicate that fatty acid polarity increases as chain length decreases. According to Nhivekar and Rathod [11], polar molecules have a strong affinity for MW, as they have a high dipole moment. These molecules adjust their polarity in the applied field, causing rotation. Thus, there is an increase in friction between the molecules, generating heat and increasing the interactions of the enzyme with the substrate [8]. In the esterification reactions, non-polar solvents with $\log P > 4$ are used. In bioprinting, the acids used have $\log P$ greater than 4 [7]. Lauric acid (12:0) has a value of 4.6, myristic acid (14:0) has a value of 6.1, and palmitic acid (16:0) has a value of 7.17, which, in both media (CH and MW), provide conditions favorable for shape memory in the bioprinting technique. Therefore, the higher productivity of lauric acid under MW compared with myristic acid and palmitic acid possibly refers to the selective heating of the more polar molecules under the influence of MW and the bioprinting technique.

For the esterification reactions of the bioprinted lipases under MW with 100 W power (Figure 3), the time was varied from 5 min to 85 min. According to the results, BCL showed the highest productivity for palmitic acid at the reaction time of 25 min (101,554.68 µmol/h·mg), with a productivity increase of approximately 20 times compared with the reactions under CH and a reduced reaction time from 24 h (CH) to 25 min (MW). This occurs because MW produces efficient internal heating through direct coupling of energy with the solvent, substrate, and catalyst molecules in the reaction mixture, leading to short reaction times and allowing good yields to be obtained [7]. Palmitic acid (16:0),

which obtained the highest productivity in this case, may have the influence of the acid chain size and the interference of the potency change.

For the esterification reactions of the bioprinted lipases under MW with 200 W power (Figure 4), the time was varied from 25 min to 85 min. According to the results, bBCL showed the highest productivity for palmitic acid at the reaction time of 25 min (58,031.25 $\mu\text{mol}/\text{h}\cdot\text{mg}$), with a productivity increase of approximately 12 times compared with the reactions under CH and a reduction of the reaction time from 24 h (CH) to 25 min (MW); however, it is observed that the productivity in the reactions with 200 W is lower compared with the productivities with 50 W and 100 W. In dynamic mode for MW, radiation is emitted with greater intensity initially and then only the minimum necessary to maintain the temperature. The high intensity of irradiation dispensed at the beginning of the reaction, when 200 W of power was used, may have compromised the conformational structure of the enzyme, which led to a decrease in productivity.

The synergy between the synthesis mediated by bioprinted lipases and the synthesis promoted by MW is an excellent method for the esterification reaction. The combination of bioprinted lipases and microwave-assisted synthesis offered several benefits, such as high throughput, adaptability of the biocatalyst under most conditions, and time-efficient synthesis.

2.2. Fourier Transform Infrared (FTIR) Spectrometric Analysis

After understanding the results of the esterification reactions under CH and MW, the verification of changes in the structure of lipases during the bioprinting process and after the reactions is important to understand the increase in productivity. Thus, to observe the changes in the secondary structures of the *Burkholderia cepacia* lipase (BCL), *Candida rugosa* lipase (CRL), and porcine pancreas lipase (PPL), FTIR analyses of amide I (1700–1600 cm^{-1}) were performed, as this region is sensitive to conformational changes [18,22]. The components of the amide I region analyzed were the β -sheet (1610–1640 cm^{-1}), random coil (1640–1650 cm^{-1}), α -helix (1650–1658 cm^{-1}), and β -turn (1660–1700 cm^{-1}) of unprinted BCL, BCL bioprinted with lauric acid, BCL bioprinted with myristic acid, BCL bioprinted with palmitic acid, and BCL after the reaction times. The spectra derived from each region were included in the Appendix A (Figures A1–A3). The results of the area (%) of the secondary structure by FTIR are seen in Tables 1–3.

Table 1. Area (%) of secondary structure by Fourier transform infrared (FTIR) spectrometric analysis (amide I region) of unprinted BCL, BCL bioprinted with lauric acid, and bioprinted BCL after reaction times under MW (50 W).

Enzyme	β -Sheet (%)	Random Coil (%)	α -Helix (%)	β -Turn (%)
Unprinted BCL	15.89	25.89	35.18	21.83
BCL Bioprinted with Lauric Acid	39.35	18.44	20.15	32.80
BCL + Lauric Acid (5 min)	25.91	26.77	31.47	33.64
BCL + Lauric Acid (10 min)	17.64	22.91	32.12	28.05
BCL + Lauric Acid (25 min)	30.53	26.47	12.01	24.86
BCL + Lauric Acid (45 min)	18.97	22.39	22.57	32.15

The results of the area (%) of the secondary structure by FTIR show that the percentage of secondary structure elements changed after bioprinting and reactions. For the unprinted BCL, the α -helix content was 35.18%. A reduced content of bBCL α -helix was found for fatty acids (lauric acid: 20.15%, myristic acid: 24.12%, and palmitic acid: 26.24%). The reduction

in the α -helix content indicates the displacement of the BCL lid, which facilitates the access of the substrate to the active site, favoring the increase in enzymatic activity [18,23,24].

Table 2. Area (%) of secondary structure by FTIR (amide I region) of unprinted BCL, BCL bioprinted with myristic acid, and bioprinted BCL after reaction times under MW (50 W).

Enzyme	β -Sheet (%)	Random Coil (%)	α -Helix (%)	β -Turn (%)
Unprinted BCL	15.89	25.89	35.18	21.83
BCL Bioprinted with Myristic Acid	19.17	32.04	24.12	23.55
BCL + Myristic Acid (5 min)	16.00	26.71	25.82	28.48
BCL + Myristic Acid (10 min)	16.33	25.72	27.65	27.43
BCL + Myristic Acid (25 min)	40.39	19.22	16.59	16.74
BCL + Myristic Acid (45 min)	13.64	15.27	20.68	46.41

Table 3. Area (%) of secondary structure by FTIR (amide I region) of unprinted BCL, BCL bioprinted with palmitic acid, and bioprinted BCL after reaction times under MW (100 W).

Enzyme	β -Sheet (%)	Random Coil (%)	α -Helix (%)	β -Turn (%)
Unprinted BCL	15.89	25.89	35.18	21.83
BCL Bioprinted with Palmitic Acid	18.71	17.18	26.24	33.94
BCL + Palmitic Acid (5 min)	11.28	14.02	40.86	43.19
BCL + Palmitic Acid (10 min)	31.12	11.56	31.18	33.81
BCL + Palmitic Acid (25 min)	24.07	31.47	17.97	25.87
BCL + Palmitic Acid (45 min)	6.96	18.48	36.65	32.01

From these results, it was observed that the reduction in the α -helix content of the bBCL varied according to the productivity results. The greater the decrease in the α -helix content, the greater the productivity of the bBCL: 198,661.73 $\mu\text{mol/h}\cdot\text{mg}$ using lauric acid, 123,614.43 $\mu\text{mol/h}\cdot\text{mg}$ using myristic acid, and 101,554.68 $\mu\text{mol/h}\cdot\text{mg}$ using palmitic acid. Thus, the more the α -helix content decreases, the greater the displacement of the lipase lid and, consequently, the more exposed the active site of the enzyme, making it easier for the substrate to access [18,25,26]. An increase in the β -sheet content of the bBCL was also observed, making the BCL structure more rigid because of the loss of intermolecular hydrogen bonds between the water molecules and the enzyme surface [18,27].

The lid opening rate after lipase activation is critical in regulating lipase catalysis. In some studies, complex lid movements were identified in some lipases as strong indicators of catalytic activity in organic media, among the *Candida antarctica* lipase B, *Yarrowia lipolytica*, *Burkholderia cepacia*, and porcine pancreas lipase. These studies have investigated the role of lids as a cover or modulator of the lipase active site, as well as their functional role in lipase catalysis [24,25,28]. For example, it was revealed that lowering the energy barrier for opening the lid promoted the activation of *Thermomyces lanuginosa* [28]. Lipases produced naturally by organisms have relatively low activities. Therefore, with the bioprinted lipases, for example, the higher productivity of the bBCL obtained in this study is a desired type of biocatalyst for industrial applications.

2.3. Operational Stability

Figure 5 shows the deactivation model fitted to the experimental results for bBCL esterification assisted by MW (50 W) along eight consecutive reuses of 25 min each. The Sadana model was fitted to the experimental results, as well as the half-life time (time required for half of the enzyme activity to be lost because of deactivation) of bBCL.

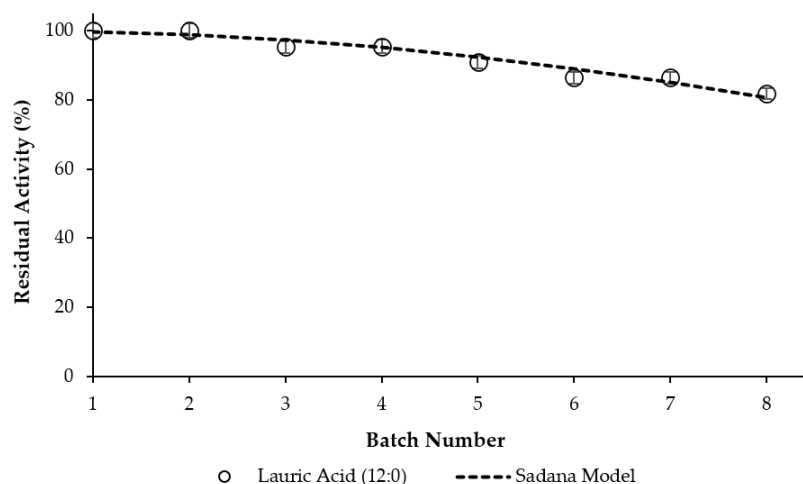


Figure 5. Batch operational stability tests for BCL bioprinted with lauric acid (12:0) during esterification assisted by microwave irradiation (50 W) at 45 °C (1 batch = 25 min).

The series-type enzyme deactivation kinetics is given by Equation (1) [29]:

$$\text{Act} = 100 - 50 \times k_d \times t^2 \quad (1)$$

where Act is the residual activity (%) at batch n, K_d is the deactivation constant, and t is time (or n-batch). In the present study, K_d was 0.00607.

The half-life of the biocatalyst, $t_{1/2}$, is estimated by Equation (2):

$$t_{1/2} = \frac{1}{\sqrt{k_d}} \quad (2)$$

where K_d is the deactivation constant and t is time.

The reuse of enzymes is an important factor that affects the cost and use in industrial applications [30,31]. bBCL reached about 81% residual activity after eight cycles, losing only 19% of its initial activity, with a half-life time of 12.8 batches, corresponding to 320.8 min (approximately 5 h). This loss in residual activity with successive reactions can be attributed, in part, to mechanical stress from magnetic stirring on the three-dimensional structure of BCL [30] or to the denaturation of BCL through undesirable enzyme–product interactions [32].

Brandão et al. [18] showed that BCL bioprinted with lauric acid maintained its original relative activity after five successive cycles of the esterification reaction because of the stability of the open conformation, which facilitated the access of the substrate to its active site. According to Li et al. [33], BCL performed in operational stability, reuse, and recycling for eight batches in the reaction of racemic 1-phenylethanol and vinyl acetate. As shown by Soni et al. [34], BCL retained 30% of the initial activity after nine cycles of use in the kinetic resolution of (*R,S*)-2-(4-[3-chloro-2-hydroxypropoxy]phenyl)acetamide.

2.4. Storage Time

The storage time of BCL bioprinted with lauric acid was determined. Figure 6 shows the relative activity for storage time of BCL bioprinted with lauric acid (12:0) assisted by

MW. The results show a gradual and slow decrease in relative activity over five weeks, maintaining $\approx 80\%$ of activity. After 6 weeks, the relative activity was $\approx 40\%$.

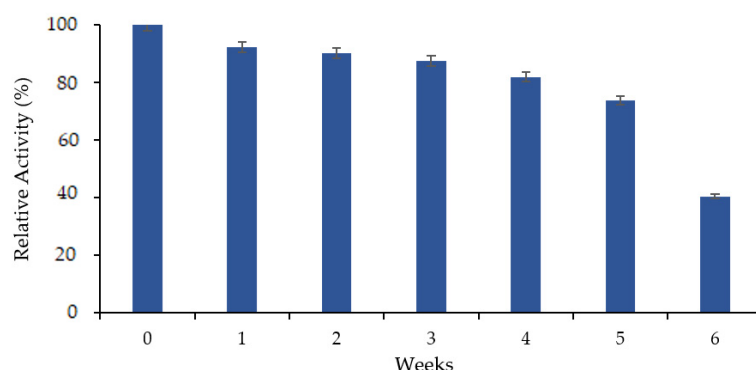


Figure 6. Storage time of BCL bioprinted with lauric acid (12:0) assisted by microwave irradiation (50 W) at 45 °C for 25 min.

The costs of enzymes and the time required to immobilize or bioprint them have created demands for enzymes with long storage stability periods. Thus, it is possible to program its application in a reaction [35]. Xu et al. [36] studied the storage time of BCL and observed that it maintains more than 80% activity after storage for 20 days. The bioprinting technique promotes greater structural rigidity of lipase [18,27], which can lead to extended storage times.

3. Materials and Methods

3.1. Materials

Lipases (*Burkholderia cepacia* lipase (BCL), *Candida rugosa* lipase (CRL), and porcine pancreas lipase (PPL)) and octane were purchased from Sigma-Aldrich (St. Louis, MO, USA). Ethyl alcohol, *n*-butanol, and fatty acids (lauric acid (12:0), myristic acid (14:0), palmitic acid (16:0), stearic acid (18:0), and oleic acid (18:1)) were purchased from Vetec Química (Sigma-Aldrich, Duque de Caxias, RJ, Brazil), Neon Comercial Ltda (Suzano, SP, Brazil), and Dinâmica Química Contemporânea Ltda (Indaiatuba, SP, Brazil).

3.2. Bioprinted with Fatty Acids

Bioprinting of BCL, CRL, and PPL with fatty acids (lauric acid (12:0), myristic acid (14:0), palmitic acid (16:0), stearic acid (18:0), and oleic acid (18:1)) was performed based on the methodology of Brandão et al. [18]. Here, 0.8 g of lipase was added to 10 mL of isopropanol and fatty acid mixture and kept under stirring at 200 rpm for 60 min at 25 °C. Subsequently, the fatty acid was removed with 20 mL of octane, and the solid was recovered and dried under vacuum at 25 °C for 24 h.

3.3. Productivity Calculation

Lipase-mediated fatty acid esterification was carried out with the same fatty acids used in the studies of Brandão et al. [18]. Free BCL, CRL, and PPL were used for the initial esterification activity analysis and the calculation of productivity [37,38].

Fatty acids (lauric acid, myristic acid, palmitic acid, stearic acid, and oleic acid) and alcohols (consisting of ethanol and butanol 1:1) [18,39–42] were used at molar ratio of 1:8. The reactions were carried out in 15 mL tubes with the volume of starting material solutions $\cong 7$ mL. The experiments started when 0.6 g of free lipase was added and stirred with a mechanical stirrer at 200 rpm at 45 °C. After 24 h, 100 μ L of sample was diluted in 4 mL of ethanol to monitor residual fatty acid levels by titration with 150 mM NaOH solution and to determine the ester conversion. The conversion (%), esterification activity (μ mol/h·g), and productivity (μ mol/h·mg) were calculated according to Equations (3), (4), and (5), respectively:

$$\text{Conversion (\%)} = \frac{FA_0 - FA_f}{FA_0} \times 100 \quad (3)$$

where FA_0 is the initial concentration of carboxylic acid (mM) and FA_f is the concentration of carboxylic acid at a certain reaction time (mM).

$$\text{Esterification activity } (\mu\text{mol/h} \cdot \text{g}) = \frac{FA_0 \times C_T}{T \times m_{\text{Bio}}} \quad (4)$$

where FA_0 is the initial carboxylic acids (μmol), C_T is the conversion of fatty acids in a certain time, T is time (h), and m_{Bio} is the total mass of biocatalyst offered (g).

$$\text{Productivity } (\mu\text{mol/h} \cdot \text{mg}) = \frac{FA_0 \times C_T}{C_{\text{Pro}} \times m_{\text{Bio}}} \quad (5)$$

where FA_0 is the initial carboxylic acids (μmol), C_T is the conversion of fatty acids in a certain time, T is time (h), C_{Pro} is the protein concentration (mg/g), and m_{Bio} is the total mass of biocatalyst offered (g).

The reactions under MW were carried out under the same reaction conditions in a microwave reactor (Model Discover SP, CEM Corporation—Matthews, NC, USA) in the dynamic mode (D), where the radiation is emitted intensely initially and then only the minimum necessary to maintain the temperature. The reactor was operated with controlled temperature (45 °C) and the evaluated parameter was the microwave power, which varied between 50 W and 200 W. An infrared sensor located at the bottom of the reactor monitored the temperature, which was controlled with air injection.

3.4. FTIR Spectrometric Analysis

Changes in the secondary structure of BCL, CRL, and PPL were investigated by vibrational spectroscopy in the FTIR region, using an Agilent Cary 630 Spectrophotometer (Agilent Technologies, Santa Clara, CA, USA). The FTIR of BCL, CRL, and PPL unprinted, bioprinted, and after the reaction times (lauric acid and myristic acid at 50 W and palmitic acid at 100 W) was performed in the amide I region (1700–1600 cm^{-1}) because this region is sensitive to conformational changes, identifying the peak frequencies through the secondary derivative and deconvoluted peaks using Origin 8.5 software. The β -sheet (1610–1640 cm^{-1}), random coil (1640–1650 cm^{-1}), α -helix (1650–1658 cm^{-1}), and β -turn (1660–1700 cm^{-1}) [43] were the evaluated components of this region. The secondary structure content was calculated from the percentage area of the individual peak in the amide I region [44,45].

3.5. Operational Stability

The operational stability of bBCL in the microwave-assisted esterification reactions was performed in consecutive 25 min batches in the reaction conditions described in Section 3.3. After each cycle, the lipase was washed with octane to remove any remaining reagents and products. Subsequently, bBCL was reused in a new cycle under the same reaction conditions. The residual fatty acid level was monitored at the end of each cycle by titration with 150 mM of the NaOH solution, and the productivity calculation was performed. The first lipase activity was taken as 100% and the relative activity is the percentage ratio of lipase activity to the initial activity. Enzyme deactivation models were fitted to experimental data, using the “solver” function from Excel for Windows, and used to estimate the half-life time of bBCL.

3.6. Storage Time

BCL was bioprinted as described in Section 3.2 and stored under refrigeration at 4 °C. The analysis of the microwave-assisted esterification activities of bBCL and the calculation of the productivity were performed (Section 3.3) and compared over the pre-defined storage times.

4. Conclusions

The use of MW in the esterification reactions of BCL bioprinted with lauric acid increased productivity by approximately 33 times compared with reactions under CH and a reduction in

reaction time from 24 h (CH) to 25 min (MW). The increase in productivity in the esterification reaction of bBCL demonstrates its activation, which occurred as a result of conformational changes to the enzyme in the bioprinting process. The changes were confirmed by FTIR analyses. The biocatalyst showed high operational stability over eight cycles. The results showed a gradual and slow decrease in relative activity of storage time over five weeks, maintaining $\approx 80\%$ of activity. Thus, the results demonstrate the prospect of a new enzymatic route to obtain hyperactive catalysts, with the use of bioprinted lipases in esterification reactions under MW, for the synthesis of esters with a view to large-scale industrial application.

Author Contributions: J.J.C.d.M. and G.L.P.d.S. (conceptualization, data handling, writing—original draft preparation, writing—review and editing); D.A.M. and L.M.d.S.B. (data handling, writing—original draft preparation); R.L.d.S. and M.M.P. (conceptualization); Á.S.L. (conceptualization, writing—review and editing, supervision); C.M.F.S. (conceptualization, methodology, data handling, writing—review and editing, resources, funding acquisition, supervision). All authors have read and agreed to the published version of the manuscript.

Funding: This work was supported by National Council for Scientific and Technological Development [CNPq], Coordination of Superior Level Staff Improvement-Brazil [CAPES]—Finance Code 001, and the Foundation for Research and Technological Innovation Support of the State of Sergipe [FAPITEC/SE].

Conflicts of Interest: The authors declare that no conflicts of interest exist regarding this work.

Appendix A

The spectra derived from the amide I region ($1700\text{--}1600\text{ cm}^{-1}$) of *Burkholderia cepacia* lipase (BCL) were the basis for calculating the area (%) of the secondary structure by Fourier transform infrared (FTIR) spectrometric analysis described in Tables 1–3.

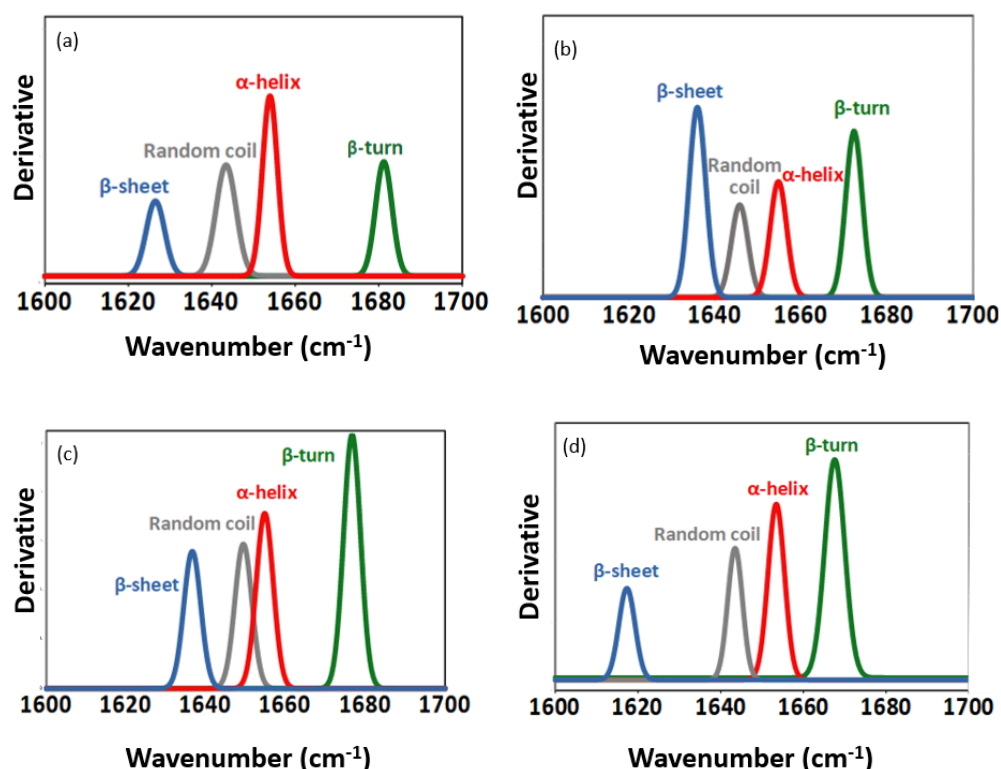


Figure A1. Cont.

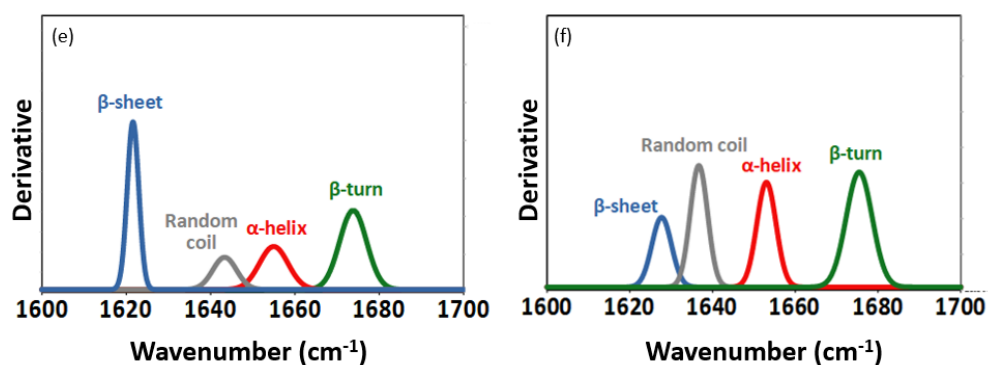


Figure A1. Spectra derived from the amide I region (1700–1600 cm⁻¹) of BCL: (a) unprinted BCL, (b) BCL bioprinted with lauric acid, and BCL bioprinted after reactions in MW at (c) 5 min, (d) 10 min, (e) 25 min, and (f) 45 min. The β-sheet is shown in blue, the random coil in gray, the α-helix in red, and the β-turn in green.

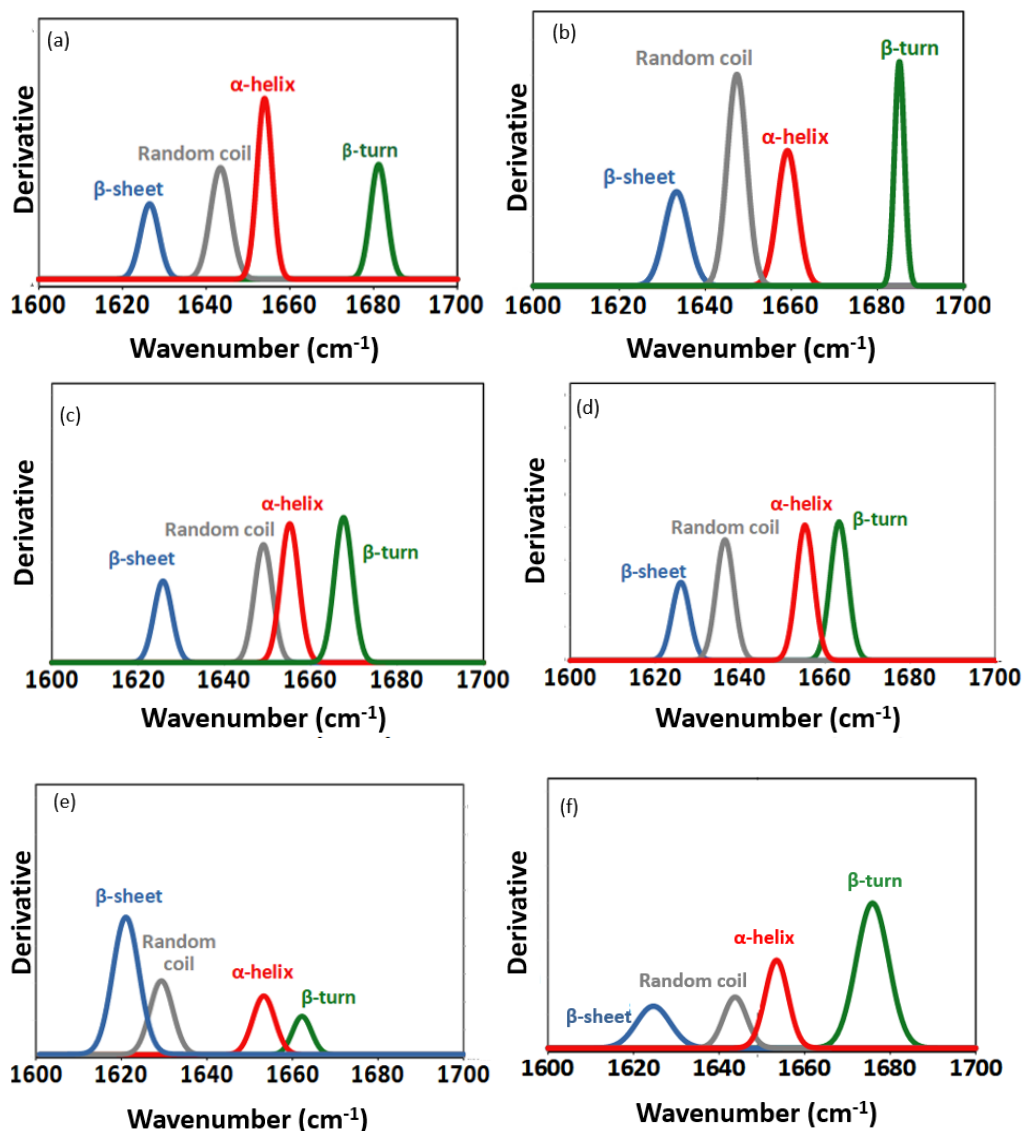


Figure A2. Spectra derived from the amide I region (1700–1600 cm⁻¹) of BCL: (a) unprinted BCL, (b) BCL bioprinted with myristic acid, and BCL bioprinted after reactions in MW at (c) 5 min, (d) 10 min, (e) 25 min, and (f) 45 min. The β-sheet is shown in blue, the random coil in gray, the α-helix in red, and the β-turn in green.

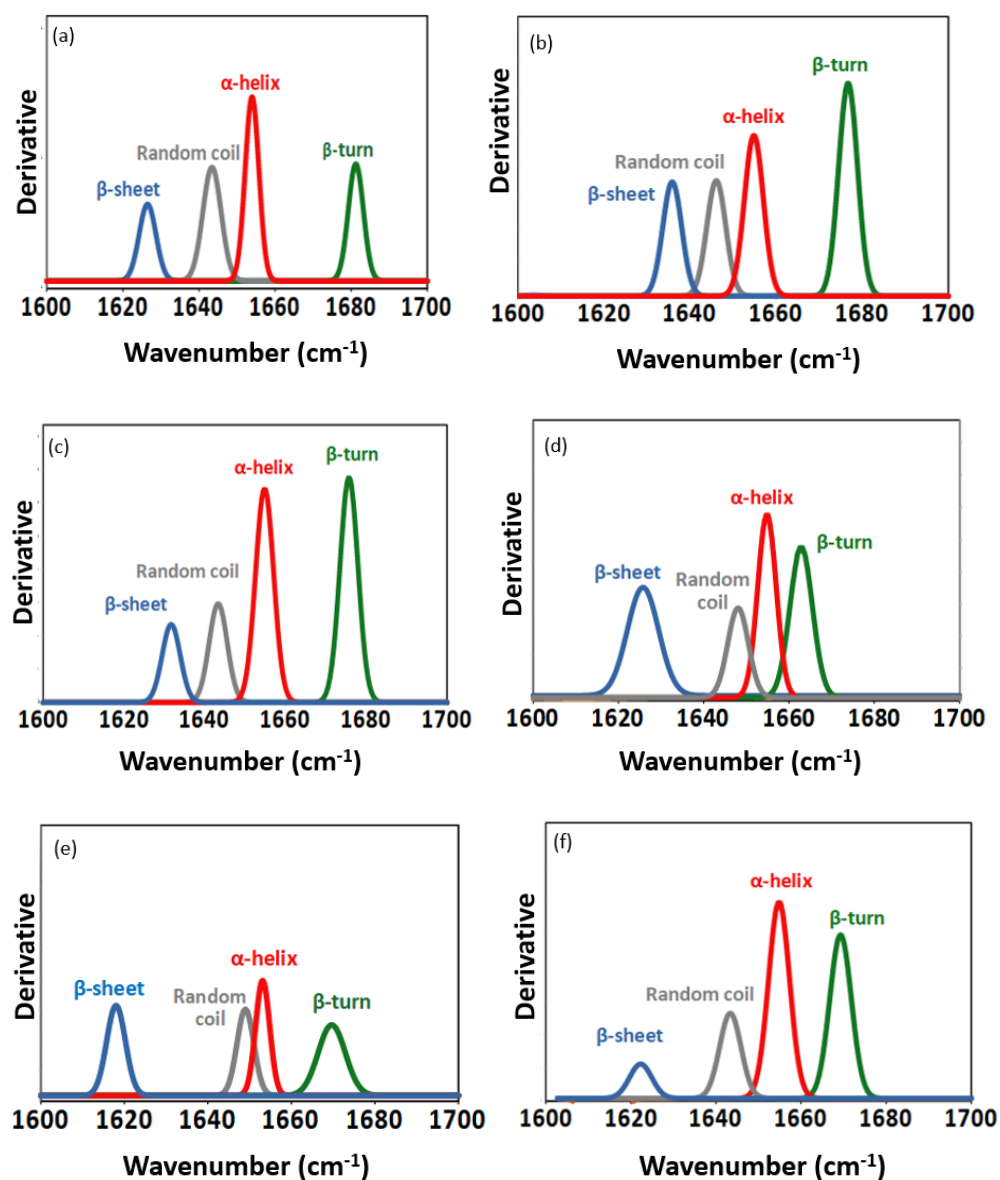


Figure A3. Spectra derived from the amide I region ($1700\text{--}1600\text{ cm}^{-1}$) of BCL: (a) unprinted BCL, (b) BCL bioprinted with palmitic acid, and BCL bioprinted after reactions in MW at (c) 5 min, (d) 10 min, (e) 25 min, and (f) 45 min. The β -sheet is shown in blue, the random coil in gray, the α -helix in red, and the β -turn in green.

References

1. Bhavsar, K.V.; Yadav, G.D. Microwave Assisted Solvent-Free Synthesis of *n*-Butyl Propionate by Immobilized Lipase as Catalyst. *Biocatal. Agric. Biotechnol.* **2018**, *14*, 264–269. [\[CrossRef\]](#)
2. Abusweireh, R.S.; Rajamohan, N.; Vasseghian, Y. Enhanced Production of Biodiesel Using Nanomaterials: A Detailed Review on the Mechanism and Influencing Factors. *Fuel* **2022**, *319*, 123862. [\[CrossRef\]](#)
3. Bukhari, A.; Idris, A.; Atta, M.; Loong, T.C. Covalent Immobilization of Candida Antarctica Lipase B on Nanopolystyrene and Its Application to Microwave-Assisted Esterification. *Chin. J. Catal.* **2014**, *35*, 1555–1564. [\[CrossRef\]](#)
4. Adak, S.; Banerjee, R. A Green Approach for Starch Modification: Esterification by Lipase and Novel Imidazolium Surfactant. *Carbohydr. Polym.* **2016**, *150*, 359–368. [\[CrossRef\]](#) [\[PubMed\]](#)
5. Das, A.; Banik, B.K. Microwave-Induced Biocatalytic Reactions toward Medicinally Important Compounds. *Phys. Sci. Rev.* **2022**, *7*, 507–538. [\[CrossRef\]](#)
6. Suo, H.; Hao, X.; Zhang, G.; Zhang, Q.; Du, S. A Kinetic Study of the Ultrasonically Assisted Ethyl Esterification of Fatty Acids Using an Immobilized Lipase Catalyst and Deep Eutectic Solvent. *Int. J. Chem. Kinet.* **2022**, *54*, 400–412. [\[CrossRef\]](#)
7. Jaiswal, K.S.; Rathod, V.K. Process Intensification of Enzymatic Synthesis of Flavor Esters: A Review. *Chem. Rec.* **2022**, *22*, e202100213. [\[CrossRef\]](#)

8. Khan, N.R.; Rathod, V.K. Microwave Mediated Lipase-Catalyzed Synthesis of *n*-Butyl Palmitate and Thermodynamic Studies. *Biocatal. Agric. Biotechnol.* **2020**, *29*, 101741. [[CrossRef](#)]
9. Khan, N.R.; Rathod, V.K. Microwave Assisted Enzymatic Synthesis of Speciality Esters: A Mini—Review. *Process Biochem.* **2018**, *75*, 89–98. [[CrossRef](#)]
10. Jaiswal, K.S.; Rathod, V.K. Microwave-Assisted Synthesis of Ethyl Laurate Using Immobilized Lipase: Optimization, Mechanism and Thermodynamic Studies. *J. Indian Chem. Soc.* **2021**, *98*, 100020. [[CrossRef](#)]
11. Nhivekar, G.S.; Rathod, V.K. Microwave-Assisted Lipase-Catalyzed Synthesis of Polyethylene Glycol Stearate in a Solvent-Free System. *J. Indian Chem. Soc.* **2021**, *98*, 100131. [[CrossRef](#)]
12. Liow, M.Y.; Gourich, W.; Chang, M.Y.; Loh, J.M.; Chan, E.S.; Song, C.P. Towards Rapid and Sustainable Synthesis of Biodiesel: A Review of Effective Parameters and Scale-up Potential of Intensification Technologies for Enzymatic Biodiesel Production. *J. Ind. Eng. Chem.* **2022**, *114*, 1–18. [[CrossRef](#)]
13. Nyari, N.L.D.; Zabet, G.L.; Zamadei, R.; Paluzzi, A.R.; Tres, M.V.; Zeni, J.; Venquiaruto, L.D.; Dallago, R.M. Activation of Candida Antarctica Lipase B in Pressurized Fluids for the Synthesis of Esters. *J. Chem. Technol. Biotechnol.* **2018**, *93*, 897–908. [[CrossRef](#)]
14. Yang, H.; Zhang, W. Surfactant Imprinting Hyperactivated Immobilized Lipase as Efficient Biocatalyst for Biodiesel Production from Waste Cooking Oil. *Catalysts* **2019**, *9*, 914. [[CrossRef](#)]
15. Chen, Z.; Huang, S.; Zhao, M. Molecularly Imprinted Polymers for Biomimetic Catalysts. *Mol. Impr. Catal.* **2016**, *11*, 229–239. [[CrossRef](#)]
16. Gutierrez, A.V.R.; Hedström, M.; Mattiasson, B. Bioimprinting as a Tool for the Detection of Aflatoxin B1 Using a Capacitive Biosensor. *Biotechnol. Rep.* **2016**, *11*, 12–17. [[CrossRef](#)]
17. Li, Z.; Liu, H.; Zhao, G.; Wang, P.; Wang, L.; Wu, H.; Fang, X.; Sun, X.; Wu, X.; Zheng, Z. Enhancing the Performance of a Phospholipase A1 for Oil Degumming by Bio-Imprinting and Immobilization. *J. Mol. Catal. B Enzym.* **2016**, *123*, 122–131. [[CrossRef](#)]
18. Brandão, L.M.S.; Barbosa, M.S.; Souza, R.L.; Pereira, M.M.; Lima, Á.S.; Soares, C.M.F. Lipase Activation by Molecular Bioimprinting: The Role of Interactions between Fatty Acids and Enzyme Active Site. *Biotechnol. Prog.* **2021**, *37*, e3064. [[CrossRef](#)]
19. Gao, J.; Yin, L.; Feng, K.; Zhou, L.; Ma, L.; He, Y.; Wang, L.; Jiang, Y. Lipase Immobilization through the Combination of Bioimprinting and Cross-Linked Protein-Coated Microcrystal Technology for Biodiesel Production. *Ind. Eng. Chem. Res.* **2016**, *55*, 11037–11043. [[CrossRef](#)]
20. de Melo, J.J.C.; Gonçalves, J.R.; Brandão, L.M.d.S.; Souza, R.L.; Pereira, M.M.; Lima, Á.S.; Soares, C.M.F. Evaluation of Lipase Access Tunnels and Analysis of Substance Transport in Comparison with Experimental Data. *Bioprocess Biosyst. Eng.* **2022**, *45*, 1149–1162. [[CrossRef](#)]
21. Mukherjee, J.; Gupta, M.N. Molecular Bioimprinting of Lipases with Surfactants and Its Functional Consequences in Low Water Media. *Int. J. Biol. Macromol.* **2015**, *81*, 544–551. [[CrossRef](#)]
22. Hoarau, M.; Badiéyan, S.; Marsh, E.N.G. Immobilized Enzymes: Understanding Enzyme-Surface Interactions at the Molecular Level. *Org. Biomol. Chem.* **2017**, *15*, 9539–9551. [[CrossRef](#)] [[PubMed](#)]
23. Alves, N.R.; Pereira, M.M.; Giordano, R.L.C.; Tardioli, P.W.; Lima, Á.S.; Soares, C.M.F.; Souza, R.L. Design for Preparation of More Active Cross-Linked Enzyme Aggregates of Burkholderia Cepacia Lipase Using Palm Fiber Residue. *Bioprocess Biosyst. Eng.* **2021**, *44*, 57–66. [[CrossRef](#)] [[PubMed](#)]
24. Miranda, J.S.; Silva, N.C.A.; Bassi, J.J.; Corradini, M.C.C.; Lage, F.A.P.; Hirata, D.B.; Mendes, A.A. Immobilization of Thermomyces Lanuginosus Lipase on Mesoporous Poly-Hydroxybutyrate Particles and Application in Alkyl Esters Synthesis: Isotherm, Thermodynamic and Mass Transfer Studies. *Chem. Eng. J.* **2014**, *251*, 392–403. [[CrossRef](#)]
25. Liu, Y.; Chen, D.; Yan, Y.; Peng, C.; Xu, L. Biodiesel Synthesis and Conformation of Lipase from Burkholderia Cepacia in Room Temperature Ionic Liquids and Organic Solvents. *Bioresour. Technol.* **2011**, *102*, 10414–10418. [[CrossRef](#)] [[PubMed](#)]
26. Pan, S.; Liu, X.; Xie, Y.; Yi, Y.; Li, C.; Yan, Y.; Liu, Y. Esterification Activity and Conformation Studies of Burkholderia Cepacia Lipase in Conventional Organic Solvents, Ionic Liquids and Their Co-Solvent Mixture Media. *Bioresour. Technol.* **2010**, *101*, 9822–9824. [[CrossRef](#)] [[PubMed](#)]
27. Qin, J.; Zou, X.; Lv, S.; Jin, Q.; Wang, X. Influence of Ionic Liquids on Lipase Activity and Stability in Alcoholysis Reactions. *RSC Adv.* **2016**, *6*, 87703–87709. [[CrossRef](#)]
28. Chen, G.; Khan, I.M.; He, W.; Li, Y.; Jin, P.; Campanella, O.H.; Zhang, H.; Huo, Y.; Chen, Y.; Yang, H.; et al. Rebuilding the Lid Region from Conformational and Dynamic Features to Engineering Applications of Lipase in Foods: Current Status and Future Prospects. *Compr. Rev. Food Sci. Food Saf.* **2022**, *21*, 2688–2714. [[CrossRef](#)]
29. Sadana, A. A Deactivation Model for Immobilized and Soluble Enzymes. *Biotechnol. Lett.* **1980**, *2*, 279–284. [[CrossRef](#)]
30. Jacob, A.G.; Wahab, R.A.; Chandren, S.; Jumbri, K.; Wan Mahmood, W.M.A. Physicochemical Properties and Operational Stability of Taguchi Design-Optimized Candida Rugosa Lipase Supported on Biogenic Silica/Magnetite/Graphene Oxide for Ethyl Valerate Synthesis. *Adv. Powder Technol.* **2022**, *33*, 103374. [[CrossRef](#)]
31. Santos, M.M.O.; Gama, R.S.; Tavares, I.M.C.; Santos, P.H.; Gonçalves, M.S.; Carvalho, M.S.; Vilas Boas, E.V.B.; Oliveira, J.R.; Mendes, A.A.; Franco, M. Application of Lipase Immobilized on a Hydrophobic Support for the Synthesis of Aromatic Esters. *Biotechnol. Appl. Biochem.* **2021**, *68*, 538–546. [[CrossRef](#)]

32. Jafarian, F.; Bordbar, A.K.; Razmjou, A.; Zare, A. The Fabrication of a High Performance Enzymatic Hybrid Membrane Reactor (EHMR) Containing Immobilized *Candida Rugosa* Lipase (CRL) onto Graphene Oxide Nanosheets-Blended Polyethersulfone Membrane. *J. Memb. Sci.* **2020**, *613*, 118435. [[CrossRef](#)]
33. Li, K.; Wang, J.; He, Y.; Cui, G.; Abdulrazaq, M.A.; Yan, Y. Enhancing Enzyme Activity and Enantioselectivity of *Burkholderia Cepacia* Lipase via Immobilization on Melamine-Glutaraldehyde Dendrimer Modified Magnetic Nanoparticles. *Chem. Eng. J.* **2018**, *351*, 258–268. [[CrossRef](#)]
34. Soni, S.; Dwivedee, B.P.; Banerjee, U.C. Facile Fabrication of a Recyclable Nanobiocatalyst: Immobilization of: *Burkholderia Cepacia* Lipase on Carbon Nanofibers for the Kinetic Resolution of a Racemic Atenolol Intermediate. *RSC Adv.* **2018**, *8*, 27763–27774. [[CrossRef](#)]
35. Gowon Jacob, A.; Abdul Wahab, R.; Misson, M.; Operational Stability, M. Operational Stability, Regenerability, and Thermodynamics Studies on Biogenic Silica/Magnetite/Graphene Oxide Nanocomposite-Activated *Candida Rugosa* Lipase Citation. *Polymers* **2021**, *13*, 3854. [[CrossRef](#)]
36. Xu, L.; Cui, G.; Ke, C.; Fan, Y.; Yan, Y. Immobilized *Burkholderia Cepacia* Lipase on pH-Responsive Pullulan Derivatives with Improved Enantioselectivity in Chiral Resolution. *Catalysts* **2018**, *8*, 13. [[CrossRef](#)]
37. Alves, M.D.; Aracri, F.M.; Cren, É.C.; Mendes, A.A. Isotherm, Kinetic, Mechanism and Thermodynamic Studies of Adsorption of a Microbial Lipase on a Mesoporous and Hydrophobic Resin. *Chem. Eng. J.* **2017**, *311*, 1–12. [[CrossRef](#)]
38. Lage, F.A.P.; Bassi, J.J.; Corradini, M.C.C.; Todero, L.M.; Luiz, J.H.H.; Mendes, A.A. Preparation of a Biocatalyst via Physical Adsorption of Lipase from *Thermomyces Lanuginosus* on Hydrophobic Support to Catalyze Biolubricant Synthesis by Esterification Reaction in a Solvent-Free System. *Enzyme Microb. Technol.* **2016**, *84*, 56–67. [[CrossRef](#)] [[PubMed](#)]
39. Santhanakrishnan, A.; Shannon, A.; Peereboom, L.; Lira, C.T.; Miller, D.J. Kinetics of Mixed Ethanol/*n*-Butanol Esterification of Butyric Acid with Amberlyst 70 and *p*-Toluene Sulfonic Acid. *Ind. Eng. Chem. Res.* **2013**, *52*, 1845–1853. [[CrossRef](#)]
40. Wu, Y.C.; Lee, H.Y.; Lee, C.H.; Huang, H.P.; Chien, I.L. Design and Control of Thermally-Coupled Reactive Distillation System for Esterification of an Alcohol Mixture Containing *n*-Amyl Alcohol and *n*-Hexanol. *Ind. Eng. Chem. Res.* **2013**, *52*, 17184–17197. [[CrossRef](#)]
41. Zhao, T.; No, D.S.; Kim, Y.; Kim, Y.S.; Kim, I.H. Novel Strategy for Lipase-Catalyzed Synthesis of Biodiesel Using Blended Alcohol as an Acyl Acceptor. *J. Mol. Catal. B Enzym.* **2014**, *107*, 17–22. [[CrossRef](#)]
42. Lamba, R.; Sarkar, S. Synergistic Effect of Mixed Alcohols on Esterification of Decanoic Acid with Amberlyst 15 as Catalyst. *Environ. Prog. Sustain. Energy* **2019**, *38*, 13103. [[CrossRef](#)]
43. Nadar, S.S.; Rathod, V.K. Sonochemical Effect on Activity and Conformation of Commercial Lipases. *Appl. Biochem. Biotechnol.* **2017**, *181*, 1435–1453. [[CrossRef](#)] [[PubMed](#)]
44. Kumar, M.M.; Kumari, S.B.; Kavitha, E.; Velmurugan, B.; Karthikeyan, S. Spectral Profile Index Changes as Biomarker of Toxicity in *Catla Catla* (Hamilton, 1822) Edible Fish Studied Using FTIR and Principle Component Analysis. *SN Appl. Sci.* **2020**, *2*, 1233. [[CrossRef](#)]
45. Shah, S.; Gupta, M.N. Simultaneous Refolding, Purification and Immobilization of Xylanase with Multi-Walled Carbon Nanotubes. *Biochim. Biophys. Acta (BBA)-Proteins Proteom.* **2008**, *1784*, 363–367. [[CrossRef](#)]

Disclaimer/Publisher’s Note: The statements, opinions and data contained in all publications are solely those of the individual author(s) and contributor(s) and not of MDPI and/or the editor(s). MDPI and/or the editor(s) disclaim responsibility for any injury to people or property resulting from any ideas, methods, instructions or products referred to in the content.